A Proposal to Jefferson Lab PAC27

Measurement of the Target Single-Spin Asymmetry in Quasi-Elastic $^3\mathbf{He}^{\uparrow}(e, e')$

(The Jefferson Lab Hall A Collaboration)

D. J. Margaziotis
California State University, Los Angeles, CA

S. Zhou
China Atomic Energy Institute, Beijing, China

D. Armstrong, T. Averett (spokesperson[a]), M. Finn, K. Griffioen, T. Holmstrom, A. Kelleher, V. Sulkosky
College of William and Mary, Williamsburg, VA

W. Chen, D. Dutta, H. Gao, K. Kramer, X. Qian, W. Xu, Q. Ye, X. Zong
Duke University, Duhram, NC

B. Bertozzi, O. Gayou, S. Gilad
Massachusetts Institute of Technology, Cambridge, MA

P. Ulmer, L. Weinstein
Old Dominion University, Norfolk, VA

R. Gilman, C. Glashausser, X. Jiang (spokesperson), E. Kuchina, R. Ransome
Rutgers University, Piscataway, NJ

A. Afanasev, J.-P. Chen (spokesperson), E. Chudakov, R. Feurbach, J. Gomez, O. Hansen, D. Higinbotham, C. W, de Jager, J. LeRose, B. Michaels,S. Nanda, B. Reitz, A. Saha
Thomas Jefferson National Accelerator Facility, Newport News, VA 23606

Lingyan Zhu
University of Illinois, Urbana-Champaign, IL

W. Korsch
University of Kentucky, Lexington, KY

S. Širca
University of Ljubljana, Slovenia

Y. Jiang, H. Lu, Y. Ye
University of Science and Technology of China, Hefei, China

G. Cates, N. Liyanage, J. Singh, W. A. Tobias
University of Virginia, Charlottesville, VA

[a]Contact person: averett@jlab.org

Abstract

We propose to measure the target single-spin asymmetry, A_y, for the neutron using the inclusive quasi-elastic $^3\mathrm{He}^\uparrow(e,e')$ reaction in Hall A with a vertically polarized ^{3}He target at $Q^2 = 1.0$ and 2.3 GeV^2. In the one-photon exchange approximation, A_y is identically zero due to time-reversal invariance. However, it is also sensitive to the two-photon exchange amplitude which can be non-zero and enters A_y through the interference between the one- and two-photon amplitudes. For large enough Q^2, where the scattering predominantly occurs from asymptotically-free partons, there are contributions from both the elastic and inelastic nucleon response during two-photon exchange. Calculation of the elastic response is straight-forward and yields an asymmetry of $A^n_{y,elas} \simeq -0.005$ for the neutron at the kinematics of this experiment. The inelastic response was recently calculated using models of Generalized Parton Distributions (GPD's) as input and is on the order of $A^n_{y,inel} \simeq -0.01$, which gives a total expected asymmetry of $A^n_y \simeq -0.015$. Two different moments, each containing two of the GPD's, are needed to fully describe the inelastic response. However for the neutron, A_y is dominated by just one of these moments that contains the GPD's, H^q and E^q, that are also related to the nucleon form factors and the total angular momentum contribution to the nucleon spin from the quarks. This experiment will be performed using the standard Hall A spectrometers and a vertically polarized ^{3}He target and will measure A^n_y with an absolute statistical uncertainty of $\delta A_y \simeq 0.0023$ at each Q^2 (15% relative to the prediction above.) This experiment will be the first to firmly establish a non-vanishing A_y, a T-odd quantity that is identically zero in the Born approximation, providing new constraints on GPD models and new information on the dynamics of the two-photon exchange process.

Contents

1 Introduction

For the past forty years, information on nucleon and nuclear structure has been obtained through the study of form factors extracted from elastic electron scattering experiments. Following a well-established formalism, the assumption of the one-photon exchange approximation (Born approximation) allows the interpretation of experimental cross sections in terms of elastic (Dirac and Pauli) form factors. The validity of this approach is based on the assumption that the two-photon-exchange contribution is negligible. However, as new precision data on cross section and polarization observables become available, the importance of two-photon exchange contributions cannot be ignored. For example, in recent measurements of the proton form factors, two sets of experimental data consistently yield very different results at large Q^2 for the ratio $\mu_p G_{Ep}/G_{Mp}$ (see e.g. Ref. [1].) Because the experiments use different experimental techniques (Rosenbluth separation versus polarization transfer) to measure the form factor ratio, they have different sensitivities to two-photon exchange corrections at large Q^2. Calculations show that a two-photon contribution which is only a few percent of the cross section is enough to bring the results into agreement [2].

In addition to explaining the form factor discrepancy, recent calculations have emphasized the direct connection between two-photon exchange and the single spin asymmetry (SSA), A_y. This asymmetry is measured through unpolarized inclusive electron scattering from a target polarized perpendicular to the scattering plane. For elastic scattering, it is expected to be zero in the one-photon exchange approximation due to time-reversal invariance, but can receive a non-zero contribution from the interference between the (real) single-photon exchange amplitude and the imaginary part of the two-photon exchange amplitude. However, a non-vanishing A_y has never been clearly observed. Experimentally this asymmetry is relatively easy to measure using the standard Hall A spectrometers and a vertically polarized ^{3}He target. Because the Born contribution is not present, measurements of A_y would provide a unique opportunity to access information about nucleon structure through the dynamics of two-photon exchange.

For large momentum transfers, two-photon exchange can be described through the scattering off individual partons in the nucleon. This is indicated by the upper diagram in Figure 1 where the lepton interacts with a single, quasi-free quark. Its contribution to A_y enters through a weighted integral of the off-forward virtual Compton scattering amplitude with two space-like photons [3,4]. The physics of the nucleon enters through the hadronic intermediate state [5], shown as the black ellipse in the upper diagram in Figure 1, which can be described as elastic (no nucleon excitation) or inelastic (excited state).

The elastic intermediate state can be exactly calculated [4] and gives an asymmetry for the proton (neutron) on the order of $A_{y,elas} = 0.009$ (-0.006) at our kinematics. At low Q^2, the inelastic contributions could be estimated by inserting specific resonances for the intermediate state. For larger Q^2, the inelastic contribution to the proton was recently calculated [4] using deep-inelastic structure functions to describe the intermediate state and gave an asymmetry on the order of $A_{y,inelas} = 0.01$. This gives a combined asymmetry for the proton on the order of $A_y = 0.02$.

In another approach, it was recently shown [5] that for $Q^2 > 1$ GeV^2, the inelastic intermediate state is directly related to moments of the Generalized Parton Distributions (GPD's) [6,7]. For the kinematics of this proposal, they predict an inelastic contribution from the neutron of $A_{y,inelas} \simeq -0.01$. The neutron is particularly interesting because A_y can be directly related to just one specific moment of the GPD's. Because the contribution from the elastic intermediate state is believed well-known, a precise measurement of A_y will provide important information on the inelastic response of the nucleon during two-photon exchange and will provide a new experimental constraint on GPD model input. Although the importance of observing A_y has

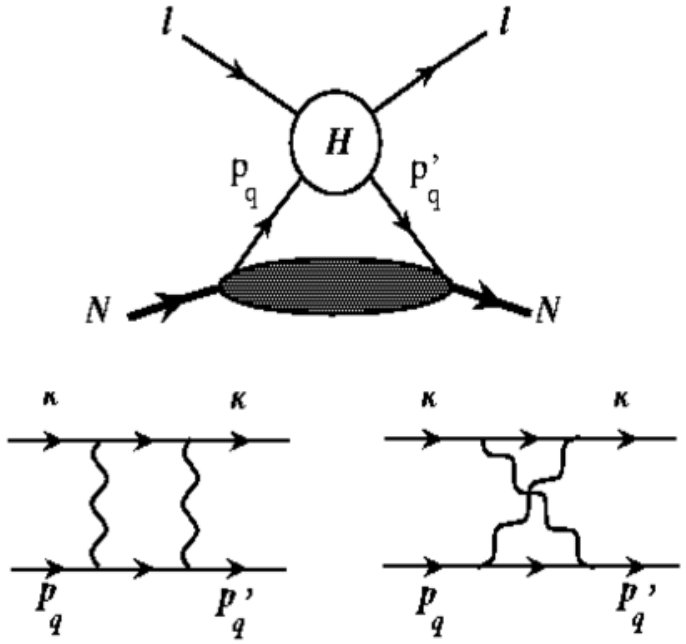

Figure 1: The upper handbag diagram shows the elastic scattering process where the lepton l with interacts at point H with a single, quasi-free quark with initial and final four-momentum p_q and p'_q. The initial and final four-momentum of the lepton are k and k', The nucleon is denoted by N and has initial and final four-momentum p and p'. The lower two diagrams show the possible two-photon exchange processes that contribute to the lepton-quark interaction at H. Figure by permission from Ref. [5].

been realized for many years, a non-vanishing A_y has never been clearly established in any experiment and it is completely unmeasured above $Q^2 = 1.0$ GeV^2.

2 The goals of this experiment

The primary goal of this experiment is to make the first measurement of A_y^n in the quasi-elastic reaction $^3\mathrm{He}^\uparrow(e,e')$ at Q^2 =1.0 and 2.3 GeV^2, with an absolute statistical uncertainty of $\delta A_y^n \simeq 0.0023$. Though an experiment on a free neutron would be ideal, for inclusive $^3\mathrm{He}^\uparrow(e,e')$ scattering, all possible hadronic final states are automatically integrated over, which means the effect of final state interactions will not generate any target single-spin asymmetry [8]. The expected asymmetry (discussed in the next section) predict neutron asymmetries $A_y^n \simeq -0.015$ at our kinematics. Given the overall (systematic and systematic) precision of this experiment, a measurement of A_y consistent with the theoretical prediction would represent a 5σ deviation from zero. This precision of this experiment will allow us to achieve three goals: 1) Clearly establish a non-zero A_y for the first time 2) provide a new experimental constraint on GPD models 3) provide quantitative information about the imaginary part of the two-photon exchange process. Together these goals will yield important information about the structure of the nucleon and the physics of the two-photon exchange process.

3 Physics Motivation

3.1 Two-photon-exchange contribution in elastic eN scattering

We consider elastic scattering of an electron, l, from a nucleon, N, described by the following kinematics,

$$l(k) \;+\; N(p) \;\rightarrow\; l(k') \;+\; N(p') \tag{1}$$

where the k (k') and p (p') are the four momenta of the incident (scattered) lepton and nucleon respectively. Under Lorentz, parity and charge conjugation invariance, the T-matrix for elastic scattering of two spin-1/2 particles can be expanded in terms of six independent Lorentz structures [9], three of them remain non-zero at the limit of $m_e \to 0$. Therefore, the T-matrix becomes:

$$\begin{aligned} T_{h,\lambda'_N\lambda_N} \;=\; & \frac{e^2}{Q^2}\,\bar{u}(k',h)\gamma_\mu u(k,h) \\ & \times\bar{u}(p',\lambda'_N)\left(\tilde{G}_M\,\gamma^\mu - \tilde{F}_2\frac{P^\mu}{M} + \tilde{F}_3\frac{\gamma\cdot K P^\mu}{M^2}\right)u(p,\lambda_N), \end{aligned} \tag{2}$$

where $h = \pm 1/2$ is the electron helicity, λ_N (λ'_N) are the helicities of the incoming (outgoing) nucleon and $K = (k+k')/2$. The quantities $\tilde{G}_M$, $\tilde{F}_2$, $\tilde{F}_3$ are complex functions of ν and Q^2, and each contains information about nucleon structure. In the Born approximation, we recover the usual electric and magnetic nucleon form factors as follows:

$$\begin{aligned} \tilde{G}_M^{Born}(\nu,Q^2) \;&=\; G_M(Q^2), \\ \tilde{F}_2^{Born}(\nu,Q^2) \;&=\; F_2(Q^2), \\ \tilde{F}_3^{Born}(\nu,Q^2) \;&=\; 0, \end{aligned} \tag{3}$$

where $F_2 = (G_E - G_M)/(1+\tau)$ and $\tau = Q^2/4M$. Since $\tilde{F}_3$ and the phases of $\tilde{G}_M$ and $\tilde{F}_2$ vanish in the Born approximation, they must originate from processes involving the exchange of at least two photons. We can separate the Born contributions from the multi-photon contributions as follows,

$$\begin{aligned} \tilde{G}_M &= G_M + \delta\tilde{G}_M \\ \tilde{F}_2 &= F_2 + \delta\tilde{F}_2 \end{aligned} \tag{4}$$

We may also use the alternative notation $\tilde{G}_E = G_E + \delta\tilde{G}_E$. Born contributions enter the expression for T at order $O(e^2)$, shown explicitly in Eq. 2. Two photon contributions enter at order $O(e^2)$ relative to the Born contribution which means they contribute to T at order $O(e^4)$. Contributions from multi-photon exchange (more than two) enter beyond $O(e^4)$ and will be treated as radiative corrections. The box diagram in Figure 1 represents the most general two-photon exchange process in elastic scattering, with the blob representing the intermediate state of the nucleon. For A_y, the crossed diagram in Figure 1 does not contribute.

3.2 Two-photon contribution to the target single-spin asymmetry A_y

An observable which is directly proportional to two-photon exchange amplitude is the asymmetry for elastic scattering of an unpolarized electron on a nucleon target polarized normal to the scattering plane (vertically polarized.)

$$A_y \;=\; \frac{\sigma^{\uparrow} - \sigma^{\downarrow}}{\sigma^{\uparrow} + \sigma^{\downarrow}}\,, \tag{5}$$

where $\sigma^{\uparrow}$ ($\sigma^{\downarrow}$) denotes the cross section for an unpolarized beam and for a nucleon spin parallel (anti-parallel) to the normal polarization vector as defined by the electron scattering plane. As shown by de Rujula *et al.*[3], this asymmetry is related to the absorptive (imaginary) part of the elastic eN scattering amplitude.

Because G_M and G_E are purely real, A_y vanishes in the Born approximation and the leading contribution arises from an interference between the one- and two-photon exchange amplitudes. Neglecting the mass of the electron and keeping terms which are of order $O(e^4)$, we can write[5],

$$\begin{aligned} A_y &= \sqrt{\frac{2\,\varepsilon\,(1+\varepsilon)}{\tau}}\;\frac{C_B(\varepsilon,Q^2)}{d\sigma} \\ &\times\left\{-G_M\,\mathcal{I}\left(\delta\tilde{G}_E+\frac{\nu}{M^2}\tilde{F}_3\right)+G_E\,\mathcal{I}\left(\delta\tilde{G}_M+\left(\frac{2\varepsilon}{1+\varepsilon}\right)\frac{\nu}{M^2}\tilde{F}_3\right)\right\}, \end{aligned} \tag{6}$$

where $\mathcal{I}$ denotes the imaginary part.

Y.-C. Chen *et al.*[5] showed that for $Q^2 > 1$ GeV^2, the hard two-photon contributions can be expressed as moments over the GPD's as follows,

$$\begin{aligned} \delta\tilde{G}_M &= C \\ \delta\tilde{G}_E &= -\left(\frac{1+\varepsilon}{2\varepsilon}\right)(A-C)+\sqrt{\frac{1+\varepsilon}{2\varepsilon}}B \\ \tilde{F}_3 &= \frac{M^2}{\nu}\left(\frac{1+\varepsilon}{2\varepsilon}\right)(A-C) \end{aligned} \tag{7}$$

with

$$\begin{aligned} A &= \int_{-1}^{1}\frac{dx}{x}K\sum_q e_q^2\,(H^q(x,0,t)+E^q(x,0,t)) \\ B &= \int_{-1}^{1}\frac{dx}{x}K\sum_q e_q^2\,(H^q(x,0,t)-\tau E^q(x,0,t)) \\ C &= \int_{-1}^{1}\frac{dx}{x}K'\sum_q e_q^2\tilde{H}^q(x,0,t) \end{aligned} \tag{8}$$

where $t=-Q^2$, K and K' contain the contributions from the hard scattering amplitudes and H^q, E^q and $\tilde{H}^q$ are the GPD's for quarks of flavor q. Combining Eqs. 6 and 7, we arrive at the following expression for A_y,

$$A_y = \sqrt{\frac{2\,\varepsilon\,(1+\varepsilon)}{\tau}}\;\frac{C_B(\varepsilon,Q^2)}{d\sigma}\left\{-G_M\,\mathcal{I}\,(B)+G_E\,\mathcal{I}\,(A)\right\}. \tag{9}$$

From this expression it is clear that a measurement of A_y will have sensitivity to GPD model input. Furthermore, for the neutron, G_E is small which means that the dominant contribution to A_y^n will come from the term containing $\mathcal{I}(B)$, providing access to one specific moment of the GPD's and making the interpretation cleaner than the proton case where both terms must be included.

In the paper by M. Guidal *et al.*[10] the GPDs are modeled using a Gaussian parameterization along with Regge behavior at low-x, multiplied by the valence quark parton distribution functions. Using this GPD model along with the two-photon formalism of Ref.[5], predictions of A_y for the neutron are shown in Figures 2 and 3 for beam energies of $E_0 = 3.3$ and 5.5 GeV, respectively. We will use this model as the basis for comparison for this experiment and will

hereafter refer to it as the "modified Regge GPD" model. For comparison, the predicted proton asymmetry at $E_0 = 3.3$ GeV is shown in Figure 4. For the proton, the expected asymmetry is smaller than the neutron and the inelastic piece contains significant contributions from the terms containing G_E^p and G_M^p, but with opposite signs.

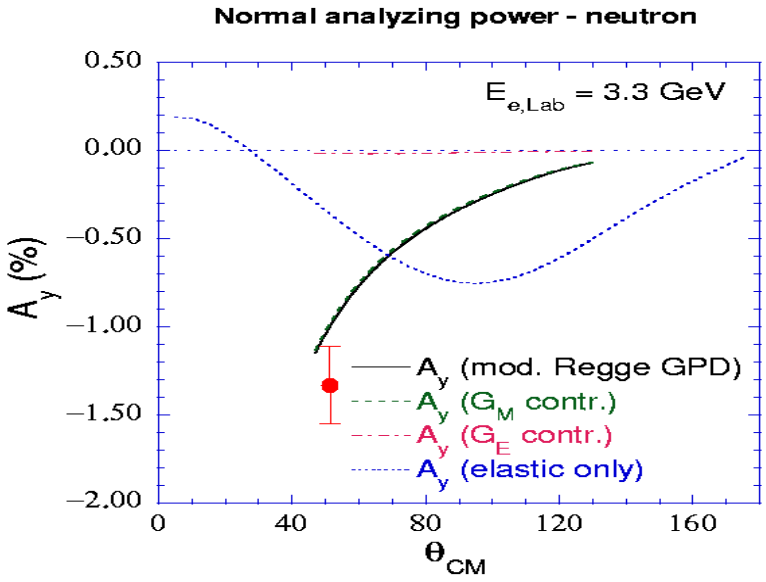

Figure 2: The normal spin asymmetry, A_y^n, for the neutron for quasi-elastic scattering as a function of the *C.M.* scattering angle for a beam energy of 3.3 GeV. The solid black curve shows the contribution from the inelastic intermediate state calculated using the modified Regge GPD as input. The elastic intermediate state contribution is shown by the dotted blue curve. The dashed (green) and dot-dash (red) curves show the individual contributions to the solid curve from the terms containing G_M and G_E respectively. The total expected asymmetry is the sum of the blue dotted and black curves. At our $\theta_{cm} = 51.1°$, the predicted asymmetry is $A_y^n = -0.0136$, shown by the red point, with the statistical uncertainty expected from this experiment.

3.3 Constraining GPD model input

As seen in Figures 2 and 3, A_y is primarily sensitive to GPD model input through the term $\mathcal{I}(B)$, that allows us to study the variation in A_y due to variations in the GPD input for H^q and E^q in the expression for B in Eq. 8. In addition, there are sum rules [6] which relate the GPDs to the Pauli and Dirac form factors,

$$F_1^q(t) = \int_{-1}^{1} dx\ H^q(x,0,t)$$
$$F_2^q(t) = \int_{-1}^{1} dx\ E^q(x,0,t), \tag{10}$$

and to J^q, the total angular momentum of the nucleon carried by a quark of flavor q

$$J^q = \frac{1}{2}\int_{-1}^{1} dx\ x\ \left[H^q(x,0,0) + E^q(x,0,0)\right]. \tag{11}$$

At $t = 0$, F_1^q must equal the total number of quarks of flavor q within the nucleon and is therefore only sensitive to the valence quark distributions. At $t = 0$, F_2^q must equal the contribution to the anomalous magnetic moment of the nucleon from a quark flavor of q. The Sachs form factors

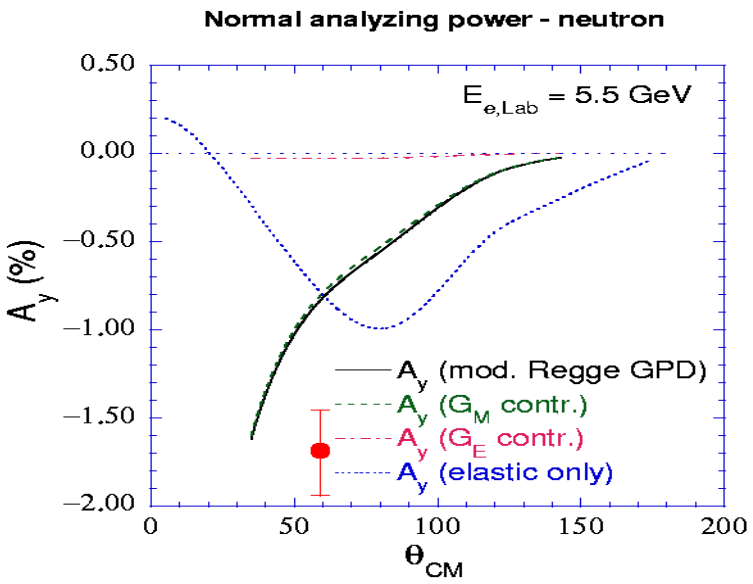

Figure 3: The normal spin asymmetry, A_y^n, for the neutron for quasi-elastic scattering as a function of the *C.M.* scattering angle for a beam energy of 5.5 GeV. The solid black curve shows the contribution from the inelastic intermediate state calculated using the modified Regge GPD as input. The elastic intermediate state contribution is shown by the dotted blue curve. The dashed (green) and dot-dash (red) curves show the individual contributions to the solid curve from the terms containing G_M and G_E respectively. At our $\theta_{cm} = 58.4°$, the predicted asymmetry is $A_y^n = -0.0171$, shown by the red point, with the statistical uncertainty expected from this experiment.

are related to the Dirac and Pauli form factors as

$$G_E(t) = F_1(t) - \tau F_2(t)$$
$$G_M(t) = F_1(t) + F_2(t). \tag{12}$$

Using the modified GPD model and Eq. 10, the world form factor data is fit to constrain the t-dependent parameters in H^q and E^q. The data are well-fit by this parameterization. A constraint also comes from Eq. 11 for J^q. The first integral in this expression may be written (assuming $q_{sea}(x) = \bar{q}(x)$),

$$\int_{-1}^{1} dx\ x\ H^q(x,0,0)\ \equiv\ \int_0^1 dx\ x\ \left[q_v(x) + 2\bar{q}(x)\right], \tag{13}$$

where q^v and $\bar{q}$ are the valence and anti-quark momentum distributions. This term is equal to the total fraction of the proton momentum carried by quark q and is reasonably well-constrained by world data on the forward parton distributions. Using the model in Ref. [6] for $E(x,0,0)$ and ignoring contributions from anti-quarks (sea quarks), predictions for J^q may be made. It is interesting to note however, that the fits to form-factor data do not provide any constraints on the anti-quark contribution to H^q and E^q. However, the moments for J_q and A_y have additional factors of x in the integrand which can give a non-zero sea quark contribution and makes them sensitive to to the choice of $\bar{q}(x)$ used. For example, to study the sensitivity in A_y to GPD model input, one could vary the sea quark contributions while still consistently fitting the form factor data. A calculation of this is currently underway [11] and will be completed by the PAC presentation.

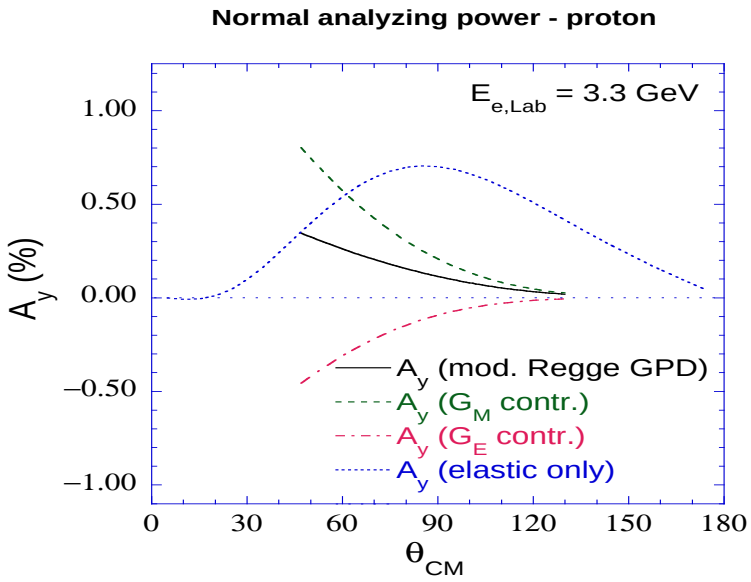

Figure 4: The normal spin asymmetry, A_y^p, for the proton for quasi-elastic scattering as a function of the *C.M.* scattering angle for a beam energy of 3.3 GeV. The solid black curve shows the contribution from the inelastic intermediate state calculated using the modified Regge GPD as input. The elastic intermediate state contribution is shown by the dotted blue curve. The dashed (green) and dot-dash (red) curves show the individual contributions to the solid curve from the terms containing G_M and G_E respectively. Note that the proton asymmetry at $\theta_c m \simeq 55^\circ$ is $A_y^p \simeq 0.006$, which is smaller than the neutron, and it receives significant contributions to the inelastic intermediate state from the G_E^p and G_M^p terms, but with opposite signs.

3.4 Validity of GPD interpretation

In order to use the GPD formalism to interpret A_y, we explicitly require that factorization holds and the handbag diagram in Figure 1 is valid. In that case, the scattering can be factorized into a hard scattering piece at H which couples the photons to the quark, and a soft contribution from the nucleon wavefunction which describes the coupling of the quark to the nucleon. In terms of the Mandelstam variables, $t = (k - k')^2$ and $s = (k + p)^2$, where the kinematics are defined in Figure 1, we require $-t$, s large. In our case, $-t = Q^2$ and $s = W^2$, the invariant mass-squared of the photon nucleon system. This ensures that the virtual photons will interact with a single quark that is essentially quasi-free. However, as $-t$ and s become small, this picture begins to fail as contributions from gluon exchange with the remainder of the nucleon, and target mass effects, become important. In the GPD formalism, because $-t$ and s are large, it is assumed that these effects can be neglected. A more realistic model will include these "higher-twist effects" in the form of quark masses, transverse quark momentum, etc.

A calculation was recently performed by A. Afanasev, C. Carlson and M. Vanderhaeghen [11] to estimate the change in A_y as the struck quark is given a mass. Here they varied the quark mass from $m_q = 0$ to $m_q = 0.45$ GeV to study the contributions from higher twist effects as the current quarks begin to dress themselves by interacting with the gluon field. Figure 5 shows the relatively small effect the inclusion of these target mass corrections has on A_y^n.

From the experimental side, there are a number of inclusive DIS experiments that indicate higher twist effects are small at $Q^2 \sim 1$ GeV^2. Two recent papers studying moments of the world data on the polarized DIS structure function g_1 for proton [12] and neutron [13] find (within uncertainties) no evidence for higher twist effects at $Q^2 = 1$ GeV^2. In Hall A, a precision measurement of the neutron DIS spin structure function g_2 at five points around $Q^2 = 1 \simeq 1.0$ GeV^2 is completed and is nearing publication [14]. The leading twist contribution to g_2 can be

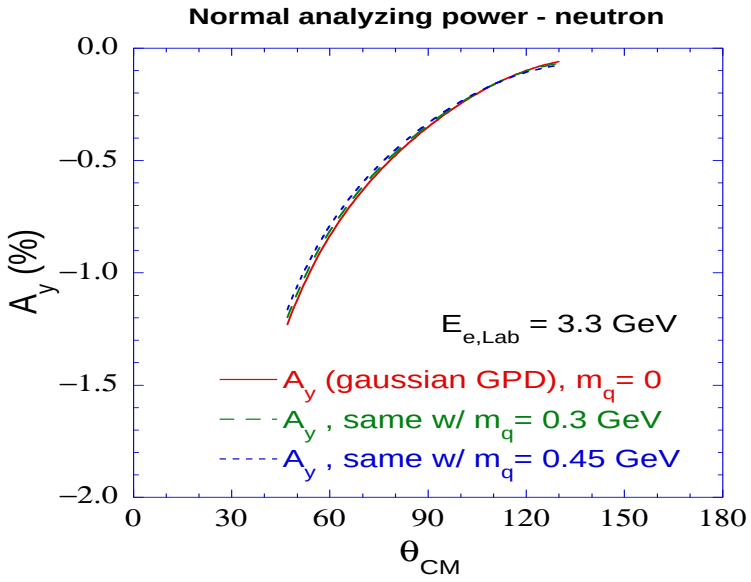

Figure 5: The normal spin asymmetry, A_y^n, for the neutron at $E = 3.3$ GeV as a function of the *C.M.* scattering angle. The different curves show the effect of including target mass corrections. There is relatively little variation in A_y^n when the quark mass is varied from 0 to 0.45 GeV.

calculated using world data on g_1. After subtracting the leading contribution, the remainder is due to higher twist effects. Preliminary results at five points around $Q^2 = 1.0$ GeV^2 indicate that the higher twist effects are non-zero, but relatively small. Global analyses [15] of unpolarized Parton Distribution Functions (PDFs) from MRST and CTEQ show no indication of higher twist effects except at large x.

In semi-incluisve DIS, it has been a concern whether factorization works at $Q^2 = 1-2$ GeV^2 at Jefferson Lab and HERMES energies. The recent data from semi-inclusive measurements in Hall B [16], Hall C [17] and HERMES [18] have shown that factorization works surprisingly well in this kinematic region.

For the Jefferson Lab Deeply Virtual Compton Scattering (DVCS) experiments (E00-100 and E03-106) [19], which are also attempting to access GPD information, a theoretical estimate was made [20] that showed the contribution from k_T (transverse quark momentum as a result of higher twist effects) is not significant for $Q^2 \simeq 2$ GeV^2. These experiments are currently running. Another completed Jefferson Lab experiment, E99-114 [21], measured the polarization transfer in real Compton scattering at $s = 6.9$ GeV^2 and $-t = 4$ GeV^2 and found that the measurement agreed best with a calculation using the handbag diagram and GPD model input. Based on this finding, a Jefferson Lab experiment known as Wide Angle Compton Scattering (E03-003 [22]) will make a new measurement at $s = 7$ GeV^2 to include four points the range $-t = 1.5 - 5.1$ GeV^2, providing additional information about factorization in our range of Q^2.

In general, if Q^2 is very large, the GPD interpretation is valid. But as Q^2 drops, higher-twist effects become increasingly important. The experiments and calculations summarized above have all indicated that higher twist effects in our Q^2 range are relatively small. These higher-twist effects are expected to enter the scattering with additional factors of $1/Q$ relative to the "pure" two-photon process. However the question of where factorization breaks down will only ultimately be determined by experiment. It is interesting to note that the predicted asymmetry for the inelastic intermediate state, with no higher twist effects included, is $A_{y,inelas} \simeq -0.01$ for both of our Q^2, while there is a factor of two change in the predicted elastic intermediate state which is believed well-known. The Q^2 dependence of our data may also provide some handle on

the size of higher twist effects if large. It will also be useful to have the data points at $Q^2 = 1.0$ and 2.3 GeV^2 when we measure A_y^n at larger Q^2 after the Jefferson Lab upgrade.

If our measured A_y is near the theoretical prediction, it gives us some confidence in the validity of the GPD model. A deviation from this prediction could be used to constrain GPD models or alternatively it could provide a constraint on the validity of the GPD interpretation at this Q^2. Both are clearly useful and interesting physics. Also note that the nucleon intermediate state can be calculated using non-GPD models such as inserting specific resonances or other inelastic contributions separately. All of these are sensitive to the structure of the neutron. In general, A_y^n is a quantity which has never been accurately measured and provides a new method to cleanly access information about the structure of the nucleon.

3.5 Existing data for A_y

In the late 1960s, an A_y measurement [24] was among the first generation of SLAC experiments. Using an electron beam with energies of 15 and 18 GeV, A_y, and the induced proton recoil polarization P_y ($A_y = P_y$ by time-reversal invariance), in the elastic ep reaction was observed to be consistent with zero up to $Q^2 = 0.98$ GeV^2 within the large experimental uncertainties, as shown in Figure 6. However, a rather small A_y is expected ($A_y < 0.005$) at the SLAC kinematics [4] due to the very forward scattering angles, $2.4^\circ < \theta^e_{lab} < 3.2^\circ$ ($13.5^\circ < \theta^e_{cm} < 19.9^\circ$), since A_y is suppressed by a kinematic factor of $\sin\theta^e_{cm}$.

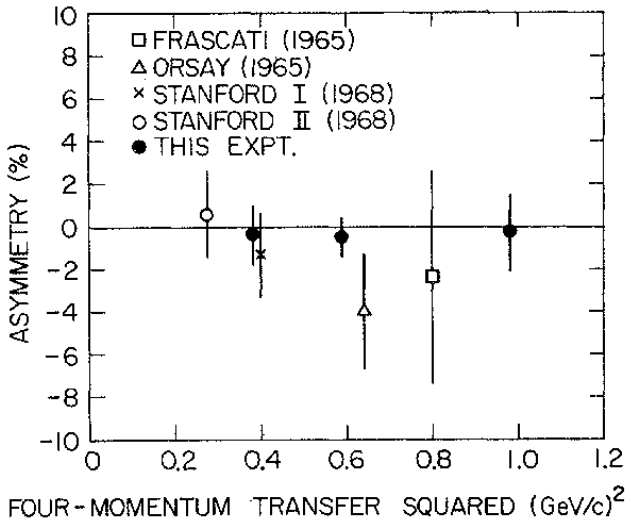

Figure 6: Data from the SLAC A_y measurements [24] referred to as "THIS EXPT." in the plot. Other data points are from measurements of the induced recoil polarization P_y. Time reversal invariance requires [3] that $P_y = A_y$. Note that A_y is consistent with zero at $Q^2 = 1.0$ GeV^2 , but the error is approximately $\pm 2\%$.

An attempt of measuring A_y in the ^{3}He(e, e') reaction at $Q^2 = 0.1$ GeV^2 was also made at NIKHEF [25]. Here, A_y for quasi-elastic scattering was found to be $A_y = -0.095 \pm 0.054$, which is 1σ from zero for the large error bars of the experiment. The asymmetry in the Δ-resonance region was measured to be $A_y = 0.029 \pm 0.055$.

3.6 Two-photon contribution to G_E^p/G_M^p

Experimentally, two independent methods have been used to determine the ratio of $R = \mu_p G_E^p/G_M^p$ assuming the Born approximation is valid. The first is the Rosenbluth method [26],

which uses measurements of the unpolarized cross section,

$$d\sigma_B = C_B(Q^2,\varepsilon)\left[G_M^2(Q^2) + \frac{\varepsilon}{\tau}G_E^2(Q^2)\right], \tag{14}$$

where ε is the photon polarization parameter, and $C_B(Q^2,\varepsilon)$ is a kinematic factor. For a fixed Q^2, one measures the cross section for different values of ε to determine the form factors G_M and G_E. The second is the polarization method where one measures the ratio of the perpendicular to parallel proton recoil polarization, P_t/P_l, with respect to its momentum direction.

$$\frac{P_t}{P_l} = -\sqrt{\frac{2\varepsilon}{\tau(1+\varepsilon)}}\frac{G_E}{G_M}. \tag{15}$$

As shown in Figure 7, the two sets of experimental data consistently yield very different results. It was pointed out that the discrepancy in G_E/G_M can be explained as a possible failure of the Born approximation when two-photon-exchange contributions are considered [2,5,27].

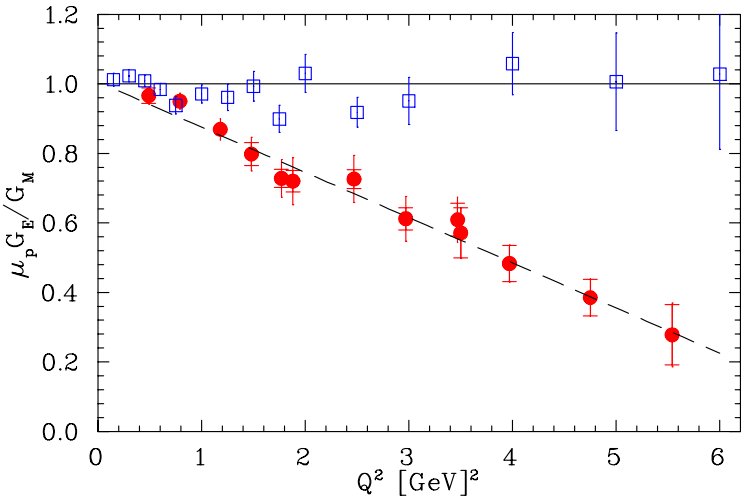

Figure 7: The existing data of $\mu_p G_E/G_M$ for proton [1] from cross section measurements [28](open squares) and from recoil polarization measurements [29,30] (solid circles).

The cross section and the recoil polarization are related to the real part of the two-photon-exchange amplitudes in different ways [2]:

$$\frac{d\sigma}{C_B(\varepsilon,Q^2)} \simeq \frac{|\tilde{G}_M|^2}{\tau}\left\{\tau + \varepsilon\frac{|\tilde{G}_E|^2}{|\tilde{G}_M|^2} + 2\varepsilon\left(\tau + \frac{|\tilde{G}_E|}{|\tilde{G}_M|}\right)\mathcal{R}\left(\frac{\nu\tilde{F}_3}{M^2|\tilde{G}_M|}\right)\right\}, \tag{16}$$

$$\frac{P_t}{P_l} \simeq -\sqrt{\frac{2\varepsilon}{\tau(1+\varepsilon)}}\left\{\frac{|\tilde{G}_E|}{|\tilde{G}_M|} + \left(1 - \frac{2\varepsilon}{1+\varepsilon}\frac{|\tilde{G}_E|}{|\tilde{G}_M|}\right)\mathcal{R}\left(\frac{\nu\tilde{F}_3}{M^2|\tilde{G}_M|}\right)\right\}, \tag{17}$$

where $\mathcal{R}$ denotes the real part, and $\tilde{G}_E = \tilde{G}_M - (1+\tau)\tilde{F}_2$.

A two-photon exchange contribution on the order of a few percent is sufficient to explain the discrepancy between the two data sets. A calculation which includes only the elastic intermediate state found that the two-photon-exchange correction has the proper sign and the magnitude to resolve a large part of the discrepancy [27]. A more recent calculation [5] of the two-photon

contribution for $Q^2 > 1$ GeV^2 included both the elastic intermediate state and the inelastic contribution. The inelastic contribution was calculated using a model of the GPD's as input. This calculation brings the data sets into agreement, indicating that the two-photon effects are sufficient to explain the discrepancy.

It is important to note that the form factor ratio is sensitive to the real part of the two-photon exchange amplitude, while A_y is sensitive to the imaginary part. So, in addition to the information we will gain on GPD's through this experiment, it will also serve as an independent verification of the two-photon formalism for the calculation of the form factor ratio. Because the models of the elastic and inelastic intermediate states (GPD's) used in calculating G_E/G_M and A_y are the same, a significant deviation from the theoretical calculation would cast doubt on the validity of two-photon exchange as an explanation for the discrepancy in the form factor ratio.

This unexpected disagreement in the form factor ratio is a perfect example of how we must begin to pay closer attention to higher order effects, such as two-photon exchange, as the precision of our experiments continues to improve with modern facilities such as Jefferson Lab. On the other hand, this improved precision also gives us the sensitivity to further explore the structure of the nucleon using new probes, such as two-photon exchange in A_y.

4 The Proposed Experiment

We plan to measure the target single-spin asymmetry A_y for the neutron in Jefferson Lab Hall A through inclusive quasi-elastic scattering from a ^{3}He target polarized normal to the scattering plane (hereafter referred to as vertically polarized.) Measurements will be made at $Q^2 = 1.0$ and 2.3 GeV^2 using an unpolarized electron beam. We plan to achieve a statistical precision of $\delta A_y^n = 0.0021$ and 0.0025 at $Q^2 = 1.0$ and 2.3 GeV^2, respectively. Based on the modified Regge GPD model, the relative precision will be $\simeq 15\%$. The vertically polarized ^{3}He target will be used in the same configuration as in the approved neutron transversity experiment, E03-004 [31]. Two HRS spectrometers on each side of the beam will be used to independently detect the scattered electrons at the same scattering angle for the $Q^2 = 1.0$ GeV^2 measurement. For the $Q^2 = 2.3$ GeV^2 measurement, only the left spectrometer will be used due to the high scattered electron momentum. No significant new equipment is needed for this experiment. The built-in cross-check of $A_y(\theta_e) = -A_y(-\theta_e)$ serves as a clear measure of systematic uncertainties at $Q^2 = 1.0$ GeV^2.

Asymmetries will be formed by flipping the polarization direction of the target every few minutes. There should be no correlation between the spectrometer detection efficiency and the target spin direction. The relative beam charge of $Q_\uparrow/Q_\downarrow$ will be determined by the regular Hall A beam charge monitors. Because we don't care about the beam polarization, we will not have to worry about charge asymmetries in the electron beam. Downstream luminosity monitor units, positioned above and below the beam pipe will count electrons from the target to provide a continuous record of the relative luminosities. The BigBite spectrometer could possibly be used at large angle as a redundant luminosity monitor.

4.1 Kinematics

The lowest value of $Q^2 = 1.0$ GeV^2 was chosen to allow us to interpret the data using GPD models where we believe the higher twist effects are still reasonably small. The upper value of $Q^2 = 2.3$ GeV^2 is the maximum we can reach while still keeping the entire run time reasonable. Guided by theoretical predictions [5], the largest A_y is expected at center-of-mass angles between $50^\circ \sim 90^\circ$.

Data will be collected at two points in Q^2 with full kinematics shown in Table 1. The expected rates and total statistical uncertainties for A_y are also listed. Two beam energies will be used, $E_0 = 3.3$ and 5.5 GeV. The respective laboratory scattering angles are 19.2° and 17.8°, corresponding to center-of-mass scattering angles of 51.1° and 58.4°. The rate and error estimates are based on a 40 cm long polarized ^{3}He target and a 15 μA beam with an average target polarization of 0.42. The expected asymmetries at $Q^2 = 1.0$ and 2.3 GeV^2 using the modified Regge model are shown in Figures 2 and 3 along with our expected statistical uncertainty.

4.2 Additional measurements

During the commissioning of the experiment, one day will be spent at $Q^2 = 0.5$ GeV^2, allowing us to achieve a statistical error comparable to the two higher Q^2 points. While this measurement will not likely be useful for constraining GPD models, it will still provide a sensitive check of the sign of the asymmetry as well as a clean check on the approximate size of the asymmetry, which has never been measured at this Q^2. Finally, it will allow us to compare the results from both spectrometers after only one day of collecting data, providing a quick measure of false asymmetries.

At the $Q^2 = 2.3$ GeV^2 point, only the left spectrometer will be used due to the momentum limitation in the right spectrometer. During this time, the right spectrometer will be set at the Δ peak to provide a check of the two-photon asymmetry from this channel. This will provide valuable information for understanding the tail of the Δ under the quasi-elastic peak. This measurement has also never been made, providing additional information about the dynamics of two-photon exchange in this channel.

E_0 (GeV)	Q^2 (GeV^2)	E' (GeV)	θ_e (deg)	θ_e^{cm} (deg)	^{3}He(e,e') rate (10^6 per day)	Time (days)	δA_y^n
3.30	0.50	3.03	12.85	35.4	405.0	1	1.2×10^{-3}
3.30	1.01	2.76	19.15	51.1	28.6	6	2.1×10^{-3}
5.50	2.26	4.30	17.80	58.4	2.3	17	2.5×10^{-3}

Table 1: Kinematics, count rates, beam time needed and the expected statistical accuracies for each setting.

4.3 The vertically polarized ^{3}He target

The vertically polarized ^{3}He target in this proposal is in the same configuration as the approved Hall A neutron transversity experiment [31]. The spokespersons for this experiment are also spokespersons on this proposal (J. P. Chen and X. Jiang) and will bring their expertise with running vertically polarized targets to this experiment. The Hall A polarized ^{3}He target has been successfully used for experiments E94-010 [32] and E95-001 [33] in 1998-1999, E99-117 [34] and E97-103 [14] in 2001 and E97-110 [35] and E01-012 [38] in 2003. The polarized ^{3}He target uses optically pumped rubidium vapor to polarize ^{3}He nuclei via spin exchange. For a 40 cm long target with target density corresponding to 10 atm at 0°C, average in-beam target polarization is about 42% with a beam current of 10-15 μA. Two kinds of polarimetry, NMR and EPR (Electron Paramagnetic Resonance), are used to measure the polarization of the target. The relative uncertainty in the polarization is typically less than $\pm$4%.

The present target configuration, with two sets of Helmholtz coils, can be polarized along any direction in the horizontal scattering plane. Two sets of diode lasers ($\approx$ 100 watts per set)

and optics are used to polarize the target along the longitudinal and the transverse directions relative to the incident electron momentum. For this experiment (and E03-004), one additional set of coils will be added for the vertical direction. With 3 sets of coils, target polarization along any direction will be possible. The horizontal coils will be oriented to avoid interference with the spectrometer entrances and the beam line.

To accommodate the vertical laser, a new oven will be built to allow laser light to impinge from the top. A conceptual design for the new target cell and oven configuration exists where the target cell will be kept the same shape as the existing target cells, but will be placed inside the scattering chamber (and target oven) with a 45° tilt to allow incident light from the top. The oven for the pumping cell will be modified to be offset with a connection piece to link with the original target ladder. The motion and target ladder system will be kept as it is now with a minor modification of an extension rod to keep the motor and any parts containing magnetic material further away from the target field region. A mirror will be mounted on top of the system such that the laser light will be reflected into the pumping cell from the top. A schematic of the target system is shown in Figure 8 for the side view and the view from beam.

It is also worth noting that the polarized target group at the College of William and Mary has now successfully filled and polarized target cells with a modified geometry that may be usable as vertically polarized cells with no tilting or modification to the existing target oven necessary.

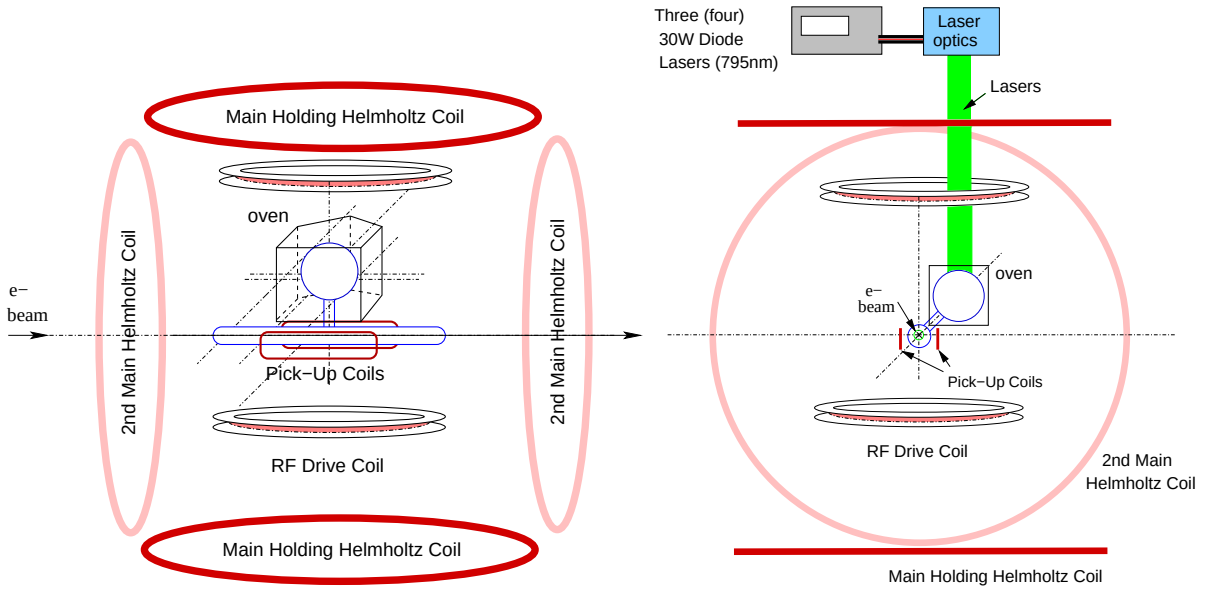

Figure 8: The schematic of the vertically polarized ^{3}He target, side view (left) and beam view (right).

The target spin needs to be flipped frequently to minimize systematic effects. The current NMR system will be modified to sweep the driving frequency through resonance at the Larmor frequency. At this time, the direction of the nucleon spins will flip by 180° relative to the holding field. By inserting (or rotating) a half-wave plate to change the polarization of the laser light, the target can continue to be polarized in the flipped spin state. It is expected that this spin flip can be accomplished in about 1 minute with minimal loss of polarization. The target spin will be flipped about once every few minutes. Each time the spins are flipped, a measurement of the target polarization is obtained from the NMR system. In addition, the EPR system can be used as needed as a second measurement of the target polarization.

The Jefferson Lab polarized ^{3}He target system has gone through upgrades and has consistently improved with time. It is maintained and operated by a mature polarized target collaboration who have been responsible for its successful operation since its inception at Jefferson Lab. A recent advance in target technology is being explored by the groups of T. Averett *et al.* at the College of William and Mary and G. Cates *et al.* at the University of Virginia. This technology, known as hybrid optical pumping, is based on the addition of potassium as an intermediate step in the polarization process [37] and is expected to provide a significant improvement in the maximum in-beam target polarization and/or polarization rate. Preliminary tests performed by these groups have proven that this technology can be scaled to work in the Jefferson Lab target systems. Further tests will soon show whether it will provide a higher overall average polarization. We are currently in the process of constructing another polarized ^{3}He target at Jefferson Lab which will be used for the upcoming measurement of G_E^n at large Q^2, E02-013 [?]. This target system will be designed to accommodate the hybrid cells and will provide useful information on the usefulness of the technique before the experiment in this proposal will run.

5 The Expected Results

Experimentally, the target single-spin asymmetry A_y is only related to the relative yields between target spin up ($\uparrow$) and spin down ($\downarrow$) configurations. Knowledge of acceptances, absolute detection efficiencies and absolute luminosities are not necessary. The measured single-spin asymmetry $A_{measured}$ can be formed from the number of events (N), corrected by the relative luminosities ($\mathcal{L}$) corresponding to target spin up and spin down runs.

$$A_{measured} = \frac{\frac{N_\uparrow}{\mathcal{L}_\uparrow} - \frac{N_\downarrow}{\mathcal{L}_\downarrow}}{\frac{N_\uparrow}{\mathcal{L}_\uparrow} + \frac{N_\downarrow}{\mathcal{L}_\downarrow}} \tag{18}$$

From the measured asymmetry $\mathcal{A}_{meas}$ the physics asymmetry, $A_y^{\rm He}$, can be obtained after corrections for the target polarization, P_T, dilution factor, η, and radiative effects, R, are applied,

$$A_y^{\rm He} = \frac{A_{meas}}{P_T \eta} R \tag{19}$$

The dilution factor corrects for scattering from the protons in ^{3}He and from unpolarized nitrogen present in the polarized target system. The neutron asymmetry is extracted by correcting for the neutron and proton polarizations in ^{3}He according to the formalism of Bissey *et al.* [39] as follows,

$$A_y^{^3{\rm He}} = \frac{\sigma^n}{\sigma^0} P_n A_y^n + \frac{\sigma^p}{\sigma^0} P_p A_y^p, \tag{20}$$

where σ^n, σ^p and σ^0 are the quasi-elastic unpolarized cross sections for neutron, proton, and the total, respectively. A corrections can also be included for a contribution from a pre-existing Δ in the nucleus. The $P_n \simeq 0.86$ and $P_p \simeq -0.028$ are the effective neutron and proton polarizations inside the nucleon. At our kinematics, $\eta \sim 0.15$. The expected statistical uncertainties from this measurement will give a 15% measurement of the modified Regge GPD prediction and are shown in Figures 2 and 3.

6 Backgrounds, Corrections and Systematic Uncertainties

6.1 Backgrounds

Because we are doing quasi-elastic inclusive scattering from vertically polarized ^{3}He, all hadronic final states are integrated over giving $A_y = 0$ for one photon exchange and time-reversal-invariant electron-photon coupling [8] This means that we will not receive any contributions from final state interactions for this process.

Other possible sources of background come from the ^{3}He elastic tail and the nucleon inelastic tail, both of which can contribute events under the quasi-elastic peak. The ^{3}He elastic tail is small at these kinematics and will not contribute significantly to the systematic error. The tail of the inelastic processes can contribute at the proposed kinematics. To estimate the size of the inelastic tail, the unpolarized cross sections are estimated using a modified QFS program [40,41] which fits the previous world data, modified to also include recent Jefferson Lab data. The model contains the following processes: the quasi-elastic scattering (QE), the Δ resonance, deep-inelastic scattering (DIS), the 2^{nd} and 3^{rd} resonances and two-nucleon processes (2N). Figures 9 and 10 show the cross sections of these processes and the total cross sections for the kinematics of the two proposed Q^2 settings. It is clear that the inelastic tail contributions increase with increasing Q^2: the total inelastic contribution at the QE peak is less than 5% at $Q^2 = 1.0$ GeV^2, and is about 20% at $Q^2 = 2.2$ GeV^2. At high Q^2 the dominant tail contribution is from the Δ resonance. The 2^{nd} resonance and the 2N processes have small contributions while the 3^{rd} resonance and the DIS processes have negligible contributions.

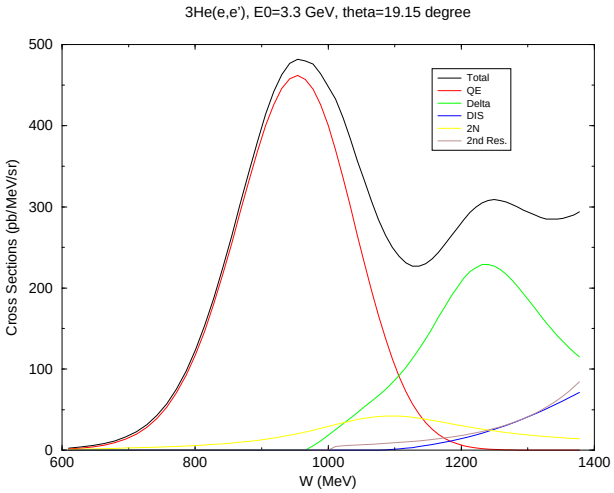

Figure 9: Relative contributions to the total unpolarized cross section for the first kinematic point at $E_0 = 3.3$ GeV and $\theta = 19.15°$ from the quasi-elastic, delta resonance, 2^{nd} resonance and two-nucleon processes.

The two-photon asymmetry A_y for the Δ is expected to be < 0.02. A calculation of this asymmetry is being carried out by A. Afanasev [23] and is expected to be ready before final submission to the PAC. The relative uncertainty of the calculation is expected to be at the level of 30%, giving a systematic uncertainty in A_y from the Δ tail contribution of $\delta A_y \simeq 2.4 \times 10^{-4}$ at $Q^2 = 1$ GeV^2 and $\delta A_y \simeq 9.0 \times 10^{-4}$ at $Q^2 = 2.2$ GeV^2.

The A_y for DIS in leading twist is expected to be proportional to m_q^2/Q^2, where m_q is the current quark mass, and therefore is negligible. The A_y for the 2^{nd} resonance and for the 2N process is expected to be in-between that for the Δ and the DIS, i.e., between ~ 0.02 to negligible. The uncertainty of the tail contributions from all other inelastic processes except the Δ resonance is therefore estimated to be less than 2×10^{-4}. So the total systematic uncertainty

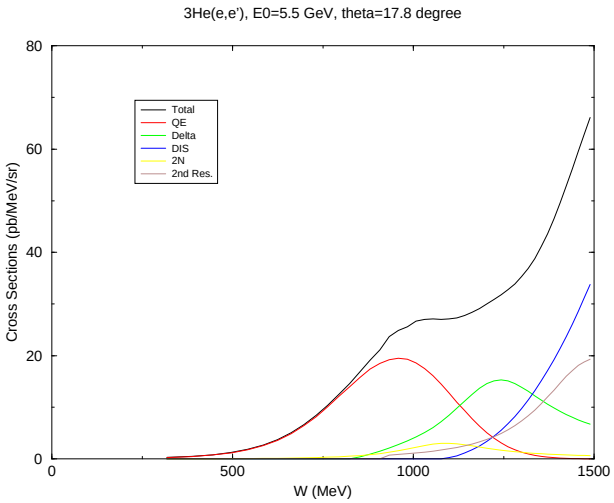

Figure 10: Relative contributions to the total unpolarized cross section for the second kinematic point at $E_0 = 5.5$ GeV and $\theta = 17.80°$ from the quasi-elastic, delta resonance, 2^{nd} resonance and two-nucleon processes.

from the inelastic tail is conservatively estimated to be $\delta A_y \simeq 4.4 \times 10^{-4}$ for $Q^2 = 1.0$ GeV^2 and $\delta A_y \simeq 1.1 \times 10^{-3}$ for $Q^2 = 2.2$ GeV^2 . Since the Δ resonance has the dominant contribution to the systematic uncertainty for the tail contributions, we plan to also measure A_y for the Δ resonance point by setting the right spectrometer (which can not be used to measure the QE due to the momentum limitation) at the peak of the Δ resonance. On the basis of this data, this systematic error may be further reduced.

6.2 Radiative corrections

External radiative corrections can be calculated using the standard prescription of Mo and Tsai[42]. In experiments where the Born contribution is dominant, two-photon exchange is treated as a radiative correction. However, for A_y, there is no Born contribution and the dominant process is from two-photon exchange. This means that the internal radiative corrections to A_y will be from physics entering at the next order beyond two-photon exchange. These corrections are expected to be small[23] relative to the external corrections. It is expected that the systematic uncertainty from radiative corrections should be no more than $\pm 3\%$ (relative to the modified Regge GPD prediction.)

6.3 Correction on A_y due to target polarization drifts

The target polarization between spin up and spin down runs may not be exactly the same. A drift in the target polarization does not cause any single-spin asymmetry itself, but results in a small change which is easy to correct.

The measured total cross section corresponding to one target spin state ($\uparrow$ or $\downarrow$) is:

$$\sigma_{\uparrow(\downarrow} = \sigma_0 \pm P_T \cdot \sigma_1, \tag{21}$$

where σ_0 and σ_1 are the target spin independent and dependent parts of ^{3}He cross section. P_T is the target polarization with a typical value of 0.4 for ^{3}He.

Ignoring radiative effects, the measured asymmetry is:

$$A_{meas} = \frac{\sigma_\uparrow - \sigma_\downarrow}{\sigma_\uparrow + \sigma_\downarrow} = P_T \frac{\sigma_1}{\sigma_0} = P_T \cdot \eta A_{phys} \tag{22}$$

where $A_{phys} = \sigma_1/\eta\sigma_0$ is the physics asymmetry for a polarized nucleon and η is the dilution factor.

The systematic uncertainty due to an uncertainty in the target polarization, δP_T, is:

$$(\delta A_{meas})_{sys} = \delta P_T \cdot \frac{\sigma_1}{\sigma_0} = \frac{\delta P_T}{P_T} \cdot A_{meas}. \tag{23}$$

If the polarization is different between the two target spin orientations, instead of Eq. 21 we have:

$$\begin{aligned} \sigma_\uparrow &= \sigma_0 + P_\uparrow \sigma_1, \\ \sigma_\downarrow &= \sigma_0 - P_\downarrow \sigma_1. \end{aligned} \tag{24}$$

The measured asymmetry becomes:

$$A_{meas} = \frac{P_\uparrow + P_\downarrow}{2} \cdot \frac{\sigma_1}{\sigma_0}. \tag{25}$$

From both Eq. 22 and Eq. 25, it is clear that drifts or systematic uncertainties in the target polarization do not generate any target single-spin asymmetry. They are second order effects only to introduce corrections or systematic uncertainties at the level of $A_{meas} \cdot \delta P_T/P_T$.

The target polarization can be determined to $\delta P_T/P_T = 4\%$ for the ^{3}He target. For a physics asymmetry of $A_{phys} = 0.02$, typical values for a polarized ^{3}He target are: $A_{meas} = 1.2\times10^{-3}$ and $(\delta A_{meas})_{sys} = \pm 3.6 \times 10^{-5}$. As long as the target polarization is measured, the drifts in average polarization between spin up and spin down runs will not cause any significant uncertainty in A_y.

6.4 The relative luminosity

Experimentally, the relative cross sections are determined from the measured event counts ($N_\pm$, corresponding to target polarization up ($\uparrow$))and down ($\downarrow$)), and the ratio of the relative integrated-luminosity, $(\mathcal{L}_+/\mathcal{L}_-)$,

$$A_{meas} = \frac{N_+ - N_- \cdot \dfrac{\mathcal{L}_+}{\mathcal{L}_-}}{N_+ + N_- \cdot \dfrac{\mathcal{L}_+}{\mathcal{L}_-}} \tag{26}$$

The systematic uncertainty on the luminosity ratio, $\delta(\mathcal{L}_+/\mathcal{L}_-)$, contributes to the systematic uncertainty of the measured asymmetry as:

$$(\delta A_{meas})_{sys} = \frac{N_- \cdot \delta\left(\dfrac{\mathcal{L}_+}{\mathcal{L}_-}\right)}{N_+ + N_- \cdot \dfrac{\mathcal{L}_+}{\mathcal{L}_-}} \cdot (1 + A_{meas}). \tag{27}$$

If we are measuring a small physics asymmetry (i.e. $N_+/\mathcal{L}_+ \approx N_-/\mathcal{L}_-$), we then have:

$$(\delta A_{meas})_{sys} \approx \frac{1}{2}(1 + A_{meas}) \cdot \frac{\delta\left(\dfrac{\mathcal{L}_+}{\mathcal{L}_-}\right)}{\dfrac{\mathcal{L}_+}{\mathcal{L}_-}}. \tag{28}$$

Eq. 28 shows that the uncertainty in the relative luminosity ratio is directly carried over into the final systematic uncertainty.

If we set the goal to control the systematic uncertainty to $(\delta A_{phys})_{sys} \leq 1 \times 10^{-3}$ while measuring a physics asymmetry of $A_{phys} = 0.02$, we need to control the ratio of the relative integrated-luminosity, $\delta(\mathcal{L}_+/\mathcal{L}_-)/(\mathcal{L}_+/\mathcal{L}_-)$, to 2×10^{-3}. Using the Hall A luminosity monitors, the uncertainty for a single measurement is 0.5%. However, we will make multiple measurements at each kinematic setting which will reduce the total uncertainty well below the level needed for this measurement.

6.5 Nuclear correction

To extract information about the neutron, we have to correct our measured asymmetries on ^{3}He for the fact that some of the scattering will occur from the effective proton polarization in ^{3}He ($P_p \simeq -0.028\%$). This is done using the formalism shown in Equation 20. The modified Regge GPD model predicts the asymmetries to be $A_y^p \simeq 0.006$ and 0.015 for $Q^2 = 1.0$ and 2.3 GeV^2, respectively. In polarized DIS measurements, this term would be small and typically would not be a large contribution to the overall systematic error. However, because we are doing quasi-elastic scattering, the unpolarized QE cross section for protons is much larger than that for neutrons. This makes us more sensitive to the uncertainty in A_y^p. We conservatively estimate that the uncertainty due to the nuclear correction to be 4.2 and 8.4% relative to the predicted A_y^n at $Q^2 = 1$ and $Q^2 = 2.3$ GeV^2 respectively, by assigning a large uncertainty to the modified Regge model for proton A_y^p.

6.6 Overall Systematic Uncertainty

Table 2 shows a conservative estimate of the expected contributions to the systematic uncertainty on A_y. The total systematic uncertainty, relative to the modified Regge GPD prediction, is estimated to be $\delta A_{y,sys} = 7 - 12\%$ with an expected statistical uncertainty of $\delta A_{y,stat} = 15\%$. The term that has a relatively large uncertainty is the the nuclear correction due to the large uncertainty in the unmeasured proton asymmetry, A_y^p. With more theoretical guidance, we have confidence we can reduce this uncertainty and have used a very conservative estimate for the error.

Source	Uncertainty in A_y (%,relative to GPD model prediction)
Target polarization	4
Nuclear correction	4-8
Radiative corrections	3
Luminosity correction	1
Inelastic background	2-6
All others	3
Total	**7-12%**

Table 2: Estimated contributions to the systematic uncertainty on A_y.

7 Proposed Beam Time

Table 3 outlines the beam time needed to complete this experiment to achieve the uncertainties in Table 1. A total of 24 days of beam on the polarized target is needed at energies of 3.3 and 5.5

GeV. An additional 4 days is needed for target spin-flips and polarimetry. Beam polarization is not needed for the A_y measurement, but if available, will allow us to look for double-spin asymmetries in the same data as by-products of this reaction.

	Time (days)
$E_0 = 3.3$ GeV	7
$E_0 = 5.5$ GeV	17
Total beam on polarized ^{3}He target	**24**
Target overhead, detector checks	**4**
Total Time Requested	**28**

Table 3: Beam time request.

8 Relation with other experiments

(1) **Jefferson Lab Experiment E03-004:**

This approved experiment will modify the existing polarized ^{3}He target system to allow for vertical polarization. Because this experiment will also measure an asymmetry, it must tackle the same problems related to systematic uncertainties from the vertically polarized target. The experiment in this proposal will be able to use this target with little modification and will also benefit from the experience gained by two of the spokespersons (J.P. Chen and X. Jiang) who are also spokespersons for this experiment.

(2) **JLab proposal PR04-008:**

This proposal shares a similar physics goal with an earlier deferred Hall C proposal PR04-008 (Polarized proton SSA in elastic ep, X. Jiang, P. Bosted, M. Jones, D. Crabb co-spokesperson). The fundamental physics idea is the same for the two proposal. The contact person and spokesperson of PR04-008, Xiaodong Jiang, is the co-spokesperson of this proposal. Many collaborators are the same for the two proposals. However, there are significant differences, mainly as a result of the choice of different polarized target. This proposal will use a high luminosity polarized ^{3}He gas target and quasi-elastic ^{3}He(e,e') reaction, while PR04-008 planned to use a vertically polarized NH_3 target.

The technical difficulties of using a vertically polarized NH_3 target make PR04-008 a rather difficult experiment with large installation efforts:

1. A new magnet with 2.5 Tesla vertical field is needed.
2. The target geometry is not the standard Hall C target geometry; significant modifications are needed.
3. Due to the low luminosity allowed by the polarized NH_3 target, two large calorimeter arrays need to be constructed to detect electron and proton.

A measurement on the neutron, using the high density polarized ^{3}He target, does not suffer from the afore-mentioned technical difficulties. In addition, there's a clear advantage of physics interpretation by the neutron measurement. The recent GPD calculation shows that the neutron SSA is dominated by one term in the GPD moments due to the small size of neutron G_E^n

form factor, while a proton measurement has contributions from two terms in GPD moments making it more complicated for a GPD interpretation.

(3) **JLab Proposal PR-04-105:**

This deferred proposal measures the single beam spin asymmetry on the proton target at low $Q^2 < 1.0$ GeV^2. It focuses on the study of the two-photon effect and trying to help resolve the discrepancy between G_E^p/G_M^p observed with recoil polarization vs. the Rosenbluth separation. Our proposal measures the single neutron (^{3}He) target spin asymmetry at $Q^2 > 1$ GeV^2, with a focus on the study of GPD's with the help of the two-photon effects.

(4) **Comments on other experiments studying GPD's:**

Other experiments with access to GPD information are: Deeply Virtual Compton Scattering (DVCS), Wide Angle Compton Scattering (WACS) and elastic form factor measurements. The study of GPD's is new and exciting and promises greater insight into the dynamics of the nucleon. But at the same time, these experiments often offer new and difficult challenges to the nuclear community. DVCS and other deep virtual exclusive reactions provide direct access to the GPDs at certain kinematic points. They are often experimentally very challenging and usually only access a rather limited kinematic coverage. Literally mapping out the multi-dimentional GPD's is currently not possible.

At present, the more practical way, is to model the GPD's with as much experimental constraint as possible. WACS and form factors experiments measure combinations of integrals (moments) of the GPDs, and provide very useful constraints in addition to the forward parton distributions extracted from DIS. However, many more experimental constraints will be needed to have a reliable 3-D picture of the nucleon. This proposed experiment is a relatively easy measurement technically and requires no new equipment. It provides clean access to a different set of moments of the GPD's and provides a unique new constraint to GPD model input. In particular, it has sensitivity to the sea part of the GPD E^q function, which is closely related to the quark orbital angular momentum through the angular momentum Sum Rule [6].

9 Collaboration

The polarized ^{3}He collaboration at Jefferson Lab has successfully completed six experiments and brings with it the necessary background and expertise for the polarized target system. No special equipment will be needed for this experiment beyond the polarized target. This experiment has been approved by the Jefferson Lab Hall A experiment.

10 Summary

In this proposal, we outline a measurement of the target single-spin asymmetry A_y in the quasi-elastic elastic ^{3}He(e, e') reaction in Hall A using a vertically polarized ^{3}He target at $Q^2 = 1.0$ and 2.3 GeV^2. The experiment can be completed in 28 days (100% efficiency) using the standard Hall A spectrometers and a vertically polarized ^{3}He target. The single-spin asymmetry A_y is sensitive to the imaginary part of the two-photon exchange amplitude and the Generalized Parton Distributions. In contrast to the proton case, the neutron is particularly useful for this measurement since it is dominated by just one moment of the GPD's. The expected uncertainties for A_y^n will be $\delta A_{y,stat} \simeq 15\%$ and $\delta A_{y,sys} \simeq 7 - 12\%$ relative to the modified Regge GPD model prediction. We will establish, for the first time, a clearly non-zero asymmetry and will provide

important quantitative information on the two-photon exchange process and nucleon structure through the GPD's.

11 Acknowledgement

We would like to thank Andrei Afanasev, Carl Carlson, Marc Vanderhaeghen, S. Brodsky and D. S. Hwang for stimulating discussions and invaluable theoretical support during the creation of this proposal.

References

1. A summary of the existing data can be found in J. Arrington, nucl-ex/0305009.
2. P.A.M. Guichon, M. Vanderhaeghen, hep-ph/03060007 and PRL.
3. A. De Rujula, J.M. Kaplan and E. De Rafael, *Nucl. Phys.* B **53**, 545 (1973).
4. A. Afanasev, I. Akushevich, N.P. Merenkov, hep-ph/0208260.
5. Y.-C. Chen *et al.*, Phys. Rev. Lett. **93**, 122301 (2004); arXiv:hep-ph/0403058.
6. X. Ji, Phys. Rev. Lett. **78** (1997) 610; Phys. Rev. D **55** (1997) 7114.
7. A. Radyushkin, Phys. Lett. B **380** (1996) 417.
8. N. Christ, T.D. Lee, Phys.Rev. **143**, 1310 (1966).
9. M.L. Goldberger, Y. Nambu and R. Oehme, Ann. of Phys. **2**, 226 (1957).
10. M. Guidal *et al.*, arXiv:hep-ph/0410251, (2004).
11. C. Carlson, M. Vanderhaeghen and A. Afanasev, private communication, to be published.
12. M. Osipenko et. al., arXiv: hep-ph/0404195 (2004). for p-n, A. Deur, et. al., Phys. Rev. Lett. 93, 212001 (2004).
13. Z.E. Meziani, et. al., arXiv:hep/ph/0404066 (2004).
14. Jefferson Lab Experiment, E97-103, URL: http://www.jlab.org/exp_prog/proposals/97/PR97-103.pdf; publication in progress.
15. A. D. Martin, R.G. Roberts, W. J. Stirling and R. S. Thorne, Eur. Phys. J. C—bf35, 325 (2004); J. Pumplin et. al., JHEP **0207**, 012 (2002), hep-ph/0201195.
16. Jefferson Lab Hall B, H. Avagyan, private comm,.
17. Jefferson Lab Hall C, R. Ent, private comm.,
18. K. Ackerstaff *et. al.*, Phys. Rev. Lett. **81**, 5519 (1998).
19. Jefferson Lab Experiment, E00-100, URL: http://www.jlab.org/exp_prog/proposals/00/PR00-100.pdf; Jefferson Lab Experiment, E03-106,
URL: http://www.jlab.org/exp_prog/proposals/03/PR03-106.pdf.
20. A. V. Radyushkin, Phys. Rev. Lett. **58**, 114008 (1998); arXiv: hep-ph/9811223 and hep-ph/0410153.
21. D.J. Hamilton *e*t al., arXiv: nucl-ex/0410001 (2004).
22. Jefferson Lab Experiment, E03-003, URL: http://www.jlab.org/exp_prog/proposals/03/PR03-003.pdf.
23. A. Afanasev, I. Akushevich and N. Merenkov, Phys. Rev. D **64**, 113009 (2001); arXiv:hep-ph/0102086; A. Afanasev, private communication.
24. T. Powell *et al.*, *Phys. Rev. Lett.* **24**, 753 (1970).
25. M. C. Harvey, Ph.D. thesis, Hampton University, 2001.
26. M.N. Rosenbluth, Phys. Rev. **79**, 615 (1950).
27. P.G. Blunden, W. Melnitchouk, J.A.Tjon, nucl-th/0306076 and PRL.
28. L. Andivahis *et al.*, Phys. Rev. D **50**, 5491 (1994).
29. M.K. Jones *et al.*, Phys. Rev. Lett. **84**, 1398 (2000).
30. O. Gayou *et al.*, Phys. Rev. Lett. **88**, 092301 (2002).

31. Jefferson Lab Experiment E03-004, URL: http://www.jlab.org/exp_prog/proposals/03/PR03-004.pdf.
32. M. Amarian *et al.*, *Phys. Rev. Lett.* **89**, 242301 (2002), and *ibid*, *Phys. Rev. Lett.* **92**, 022301 (2004).
33. W. Xu *et al.*, *Phys. Rev. Lett.* **85**, 2900 (2000), and F. Xiong *et al.*, *Phys. Rev. Lett.* **87**, 242501 (2001).
34. X. Zheng *et al.*, *Phys. Rev. Lett.* **92**, 012004 (2004); arXiv: nucl-ex/0405006.
35. Jefferson Lab Experiment, E97-110,
URL: http://www.jlab.org/exp_prog/proposals/97/PR97-110.pdf.
36. Jefferson Lab Experiment, E01-012,
URL: http://www.jlab.org/exp_prog/proposals/01/PR01-012.pdf.
37. E. Babcock *et al.*, *Phys. Rev. Lett.* **91**, 123003 (2003).
38. Jefferson Lab Experiment, E02-013,
URL: http://www.jlab.org/exp_prog/proposals/02/PR02-013.pdf.
39. F. Bissey *et al.*, Phys. Rev. C**65**, 064317 (2002).
http://hallaweb.jlab.org/physics/experiments/he3/gdh/index.html.
40. J. W. Lightbody Jr. and J. O'Connell, Computers in Physics May/June, 57 (1988).
41. K. Slifer, "Spin Structure of 3He and the Neutron at Low Q^2; A Measurement of the Extended GDH Integral and the Burkhardt-Cottingham Sum Rule", Ph. D thesis, Temple University, (2004).
42. L. Mo and Y.-S. Tsai, Rev. Mod. Phys. **41**, 205 (1969).